Role of post-translational modifications at the β-subunit ectodomain in complex association with a promiscuous plant P4-ATPase

Sara R. Costa*, Magdalena Marek*[1], Kristian B. Axelsen*†, Lisa Theorin*, Thomas G. Pomorski*‡ and Rosa L. López-Marqués*[2]

*Department of Plant and Environmental Sciences, Centre for Membrane Pumps in Cells and Disease-PUMPKin, University of Copenhagen, DK-1871, Frederiksberg C, Denmark
†SIB Swiss Institute of Bioinformatics, CMU, CH-1211, Geneva, Switzerland
‡Faculty of Chemistry and Biochemistry, Department of Molecular Biochemistry, Ruhr University Bochum, Universitätstrasse 150, D-44780 Bochum, Germany

P-type ATPases of subfamily IV (P4-ATPases) constitute a major group of phospholipid flippases that form heteromeric complexes with members of the Cdc50 (cell division control 50) protein family. Some P4-ATPases interact specifically with only one β-subunit isoform, whereas others are promiscuous and can interact with several isoforms. In the present study, we used a site-directed mutagenesis approach to assess the role of post-translational modifications at the plant ALIS5 β-subunit ectodomain in the functionality of the promiscuous plant P4-ATPase ALA2. We identified two N-glycosylated residues, Asn^{181} and Asn^{231}. Whereas mutation of Asn^{231} seems to have a small effect on P4-ATPase complex formation, mutation of evolutionarily conserved Asn^{181} disrupts interaction between the two subunits. Of the four cysteine residues located in the ALIS5 ectodomain, mutation of Cys^{86} and Cys^{107} compromises complex association, but the mutant β-subunits still promote complex trafficking and activity to some extent. In contrast, disruption of a conserved disulfide bond between Cys^{158} and Cys^{172} has no effect on the P4-ATPase complex. Our results demonstrate that post-translational modifications in the β-subunit have different functional roles in different organisms, which may be related to the promiscuity of the P4-ATPase.

Key words: *Arabidopsis thaliana*, Cdc50 ectodomain, disulfide bond, flippase, N-glycosylation.

INTRODUCTION

The P-type ATPase superfamily comprises a large number of primary transmembrane-spanning transporters that share the common characteristic of forming a phosphorylated intermediate during their catalytic cycle [1]. P-type ATPases are divided into five subfamilies according to their transport specificity [2]. Members of the P1, P2 and P3 subfamilies transport monovalent or divalent cations across cellular membranes. In contrast, P4-ATPases are phospholipid transporters necessary to create and maintain an asymmetrical distribution of phospholipids in eukaryotic plasma membranes and membranes of the late secretory and endocytic compartments [3]. Finally, P5-ATPases are eukaryotic proteins with no assigned specificity, although a human member of this family has been suggested to transport polyamines [4]. Within the large and heterogeneous P-type ATPase superfamily, only the P2C- and P4-ATPase subfamilies are known to require a heterodimeric interaction with a β-subunit [5,6]. Although P2C- and P4-ATPase β-subunits do not share sequence similarity, they are alike in terms of polypeptide chain length and membrane topology [5,6], and they seem to fulfil similar functional roles, being required for maturation, ER (endoplasmic reticulum) exit, subcellular trafficking and catalytic activity of the P-type ATPase [6–16].

The β-subunits of P4-ATPases belong to the evolutionarily conserved family of the Cdc50 (cell division control 50) proteins [17,18]. The number of Cdc50 isoforms appears to differ between organisms. Whereas only one isoform has been described in *Caenorhabditis elegans* [17], three isoforms are present in yeast, humans and the unicellular parasite *Leishmania*, and up to five exist in plants. Some P4-ATPases interact specifically with only one β-subunit isoform, whereas others are more promiscuous and can interact with several isoforms. Monogamous P4-ATPases have been described in unicellular organisms such as yeast or *Leishmania* [9,11,19] and also in humans, where at least one P4-ATPase, ATP8A2 expressed in neurons and rod outer segments of the eye, interacts only with CDC50a [20,21]. In contrast, other human P4-ATPases, such as ATP8B1 and ATP8B2, are promiscuous and can interact with both CDC50a and CDC50b [7,20]. This also seems to be the case for plant P4-ATPases. In the model plant *Arabidopsis thaliana*, all P4-ATPases analysed to date can make use of any of three β-subunits for ER exit and functionality [10,22–24].

Cdc50 proteins are a bit smaller than 400 amino acids in length and present two transmembrane spans separated by a large exoplasmic loop, which contains two to four glycosylation sites and is stabilized by disulfide bonds [7,18,21,25–27]. The role of post-translational modification of the β-subunit in P4-ATPase functionality is poorly studied. In yeast, disruption of each of two disulfide bonds in the ectodomain of the P4-ATPase β-subunit Lem3p has opposite effects on trafficking of the complex and lipid translocation [17]. Mutation of any of the cysteine residues

Abbreviations: CDC50, cell division control 50; DDM, n-dodecyl-β-maltoside; ER, endoplasmic reticulum; mPEG, methoxypolyethylene glycol-5000 maleimide; NBD-PC, 1-palmitoyl-2-[6-(7-nitrobenz-2-oxa-1,3-diazol-4-yl)amino]hexanoyl-*sn*-glycero-3-phosphocholine; NBD-PE, 1-palmitoyl-2-[6-(7-nitrobenz-2-oxa-1,3-diazol-4-yl)amino]hexanoyl-*sn*-glycero-3-phosphoethanolamine; NBD-PS, 1-palmitoyl-2-[6-(7-nitrobenz-2-oxa-1,3-diazol-4-yl)amino]hexanoyl-*sn*-glycero-3-phosphoserine; PC, phosphatidylcholine; PE, phosphatidylethanolamine; PI, propidium iodide; PNGase F, peptide N-glycosidase F; POPC, 1-palmitoyl-2-oleoyl-*sn*-glycero-3-phosphocholine; POPS, 1-palmitoyl-2-oleoyl-*sn*-glycero-3-phospho-L-serine; PS, phosphatidylserine; SD, synthetic glucose; SG, synthetic galactose; TCA, trichloroacetic acid.

[1] Present address: Department of Fundamental Microbiology, University of Lausanne, CH-1015 Lausanne, Switzerland.
[2] To whom correspondence should be addressed (email rlo@plen.ku.dk).

involved in formation of the first disulfide bond (closest to the N-terminus) affects interaction between complex subunits, but does not have an effect on lipid transport at the plasma membrane. In contrast, disruption of the second disulfide bond, formed between highly conserved cysteine residues, results in a reduced lipid-translocating activity, but does not seem to affect the strength of the P4-ATPase–β-subunit interaction. Whether this is also true for P4-ATPases in other organisms is not known. Studies on the effect of β-subunit N-glycosylation on P4-ATPase complex functionality in humans and parasites show contradictory results, suggesting specific organismal differences. In the unicellular parasite *Leishmania infantum,* N-glycosylation of a single specific residue (Asn^{176}), evolutionarily conserved among parasites, yeast and humans, affects lipid translocation but not trafficking of the P4-ATPase–β-subunit complex [27]. In contrast, mutation of the same N-glycosylated residue in a mammalian Cdc50 protein reduces expression levels of the P4-ATPase complex, but does not affect its ATPase activity [21]. In agreement with this, a yeast P4-ATPase does not seem to require full glycosylation of its β-subunit to form a phosphorylated intermediate during the catalytic cycle [16], but the effect of this post-translational modification on protein stability or complex assembly and trafficking in yeast remains to be elucidated.

One common characteristic of all P4-ATPase–β-subunit complexes analysed to date is that they are formed by a monogamous P4-ATPase interacting only with a specific β-subunit. In the present study, we investigated the effects of post-translational modifications at the β-subunit ectodomain on the functionality of a promiscuous P4-ATPase. As a model, we used the complex formed between the *A. thaliana* P4-ATPase ALA2 and the β-subunit ALIS5, which has been characterized previously as a pre-vacuolar compartment PS (phosphatidylserine)-specific transporter [24]. Using a site-directed mutagenesis approach, we mapped residues subjected to N-glycosylation and involved in disulfide bond formation in the ectodomain of ALIS5, and assessed their role in P4-ATPase expression, complex formation, trafficking and functionality. In contrast with other organisms, elimination of a conserved N-glycosylation site in ALIS5 affects complex formation, whereas elimination of a conserved disulfide bond does not have any consequence for the lipid-translocating activity of the complex. Our results demonstrate that conserved post-translational modifications have different functional roles in different organisms, which may be related to the promiscuous nature of the P4-ATPase.

MATERIALS AND METHODS

Yeast strain and growth conditions

Functional complementation and lipid translocation assays were carried out employing *Saccharomyces cerevisiae* mutant strain ZHY709 (*MATα his3 leu2 ura3 met15 dnf1Δ dnf2Δ drs2::LEU2*) [28]. Yeast cells were transformed using the lithium acetate method [29] and grown in rich synthetic medium containing 0.7 % (w/v) yeast nitrogen base, 2 % (w/v) glucose (SD, synthetic glucose) or galactose (SG, synthetic galactose), supplemented with 1.4 g/l yeast synthetic dropout medium lacking histidine and uracil or 1.92 g/l yeast synthetic dropout medium lacking uracil (Sigma–Aldrich). When appropriate, standard rich YPG medium [2 % (w/v) peptone, 1 % (w/v) yeast extract and 2 % (w/v) galactose] was used. For solid medium, 2 % (w/v) agar was added. For complementation assays, fresh yeast transformants were incubated in liquid SG medium for 4 h at 30 °C with shaking at 150 rev./min. For complementation tests of N-glycosylation mutants, transformants were diluted in water to a D_{600} of 0.1, 0.01, and 0.001. Drops (5 μl) were spotted on to plates. When stated, SG medium was supplemented with papuamide A (Lynsey Huxham, Flintbox) or duramycin (Sigma–Aldrich) to final concentrations of 0.05 μg/ml and 1.6 μM respectively. For complementation tests of cysteine mutants, transformants were diluted with water to a D_{600} of 0.1 and 4 μl drops were then spotted on to SD or SG control plates or on to SG gradient plates containing maximum concentrations of 0.35 μg/ml papuamide A or 2 μM duramycin. Gradient plates were prepared as described previously [30] except that they were incubated for 2 days before use to allow vertical diffusion of the toxin. All spotted plates were incubated at 30 °C for 3–4 days and experiments were repeated independently at least three times.

DNA cloning

Primers and plasmids used are listed in Supplementary Tables S1, S2 and S3. All PCRs were carried out using Phusion® High-Fidelity DNA Polymerase (New England Biolabs) according to the manufacturer's instructions. To create a FLAG-tagged ALIS5 for yeast expression studies, a modified version of pRS423-GAL [31] was constructed. The pRS423-GAL plasmid was used as a template in a PCR using primers oli2761 and oli2763. This generated a *GAL1-10* promoter fragment flanked by BamHI and EcoRI sites, and containing a FLAG tag at the *GAL1* side. The PCR fragment was cloned into pCR™4 Blunt-TOPO® using the Zero Blunt® TOPO® PCR Cloning Kit for Sequencing (Invitrogen), to generate plasmid pMP3072. The FLAG-containing *GAL1-10* fragment was excised from this plasmid with EcoRI and BamHI and ligated to pRS423-GAL digested with the same enzymes, rendering pMP3074. pMP3119 was produced by transferring the full-length *ALIS5* cDNA from pMP2022 [10] to pMP3074 after BamHI/SacI digestion. FLAG-tagged *ALIS5* was excised from pMP3119 with AgeI and SacI and ligated to pRS426-GAL [31] cut with the same enzymes, rendering a yeast multicopy plasmid containing a FLAG-tagged version of *ALIS5* and a *URA3* cassette (pMP3836).

All *alis5* mutants were generated through a homologous recombination strategy in which a number of overlapping PCR fragments were transformed into yeast strain ZHY709 together with a linearized plasmid. In most cases, two overlapping fragments containing the desired mutation(s) were generated by PCR amplification using the templates and primers listed in Supplementary Table S3. The fragments contained a 20-nt overlap with the sequence of either the *GAL1-10* promoter or the T3 annealing region of yeast plasmid pRS426-GAL. In the case of double or quadruple cysteine mutants, three overlapping fragments were generated. Aliquots of 20 μl of each PCR product were transformed without purification into yeast strain ZHY709 together with plasmid pRS426-GAL linearized with BamHI. Transformed cells (three to five colonies) were grown in 6 ml of SD medium for 24 h at 30 °C with shaking at 120 rev./min. For plasmid DNA extraction from yeast, a modification of the GenElute™ Plasmid Miniprep Kit (Sigma–Aldrich) was used. Briefly, cells were resuspended in 225 μl of resuspension buffer and 100 μl of acid-washed glass beads (0.5 mm) and 225 μl of lysis buffer were added. Cells were vortex-mixed for 30–40 min and left to stand at 4 °C for 10 min, before collecting 400 μl of cell lysate and proceeding according to the manufacturer's instructions. Plasmids were then amplified in *Escherichia coli* and sequenced. For tobacco transient expression studies, *alis5* mutant sequences were amplified by PCR using primers oli4091 and oli4092, and cloned into the pENTR™/D-TOPO® vector using

the pENTR™/D-TOPO® cloning kit (Invitrogen). *alis5* mutant versions were then transferred into plant binary plasmid pMDC32 [32] or pEarleyGate 101 [33] using the Gateway® technology. Constructs in pEarleyGate 101 contain the *alis5* DNA sequences out of frame with respect to YFP resulting in untagged proteins.

NBD (7-nitrobenz-2-oxa-1,3-diazol-4-yl)-lipid translocation assays and flow cytometry

NBD-PC {1-palmitoyl-2-[6-(7-nitrobenz-2-oxa-1,3-diazol-4-yl)-amino]hexanoyl-*sn*-glycero-3-phosphocholine}, NBD-PE {1-palmitoyl-2-[6-(7-nitrobenz-2-oxa-1,3-diazol-4-yl)amino]hexanoyl-*sn*-glycero-3-phosphoethanolamine and NBD-PS {1-palmitoyl-2-[6-(7-nitrobenz-2-oxa-1,3-diazol-4-yl)-amino]hexanoyl-*sn*-glycero-3-phosphoserine} (Avanti Polar Lipids) stocks (4 mM) were prepared in DMSO. NBD-lipid uptake experiments were performed as described previously [24]. Flow cytometry of NBD-labelled cells was performed on a Becton Dickinson FACSCalibur flow cytometer (BD Immunocytometry Systems) equipped with an argon laser and Cell Quest software (BD Biosciences). Before analysis 10^7 cells were labelled with 1 μl of 1 mg/ml PI (propidium iodide) for staining of non-viable cells. A total of 20000 cells were analysed without gating during the acquisition. Viable cells were selected on the basis of forward/side-scatter gating and PI exclusion. NBD fluorescence of living cells was plotted on a histogram and the geometric mean fluorescence intensity was used for further statistical analysis. Data analysis was performed using Cyflogic software (CyFlo).

Yeast membrane preparation and protein quantification

Yeast transformants were inoculated in 4 ml of SD medium and grown at 28 °C with shaking at 140 rev./min. After 24 h, cells were inoculated into 200 ml of SD medium and grown for 24 h under the same conditions. Cells were harvested and induced for protein expression in 1 litre of YPG medium at 24 °C with shaking at 140 rev./min. After 18–19 h of induction, cells were collected by centrifugation at 3000 ***g*** for 5 min at 4 °C and washed in 25 ml of ice-cold water. After centrifugation, cells were resuspended in 10 ml of lysis buffer [40 mM Hepes/NaOH, pH 7.5, 150 mM NaCl, 26 % (v/v) glycerol, 0.1 mM PMSF, 1 μg/ml aprotinin, 1 μg/ml leupeptin, 1 μg/ml pepstatin A, 5 μg/ml antipain and 157 μg/ml benzamidine HCl (Sigma–Aldrich)] and vortex-mixed with glass beads (200 μm; Sigma–Aldrich). The cell lysate was clarified by two consecutive centrifugation steps at 1000 ***g*** for 10 min at 4 °C and 10000 ***g*** for 15 min at 4 °C. Membranes were subsequently collected by centrifugation at 125000 ***g*** for 1 h at 4 °C. Pellets were homogenized in 1.5 ml of S-buffer (same as lysis buffer but containing 20 % (v/v) glycerol) and the protein concentration was measured spectrophotometrically using a Nanodrop™ 1000 instrument (Thermo Fisher Scientific). Total yeast membranes were snap-frozen in liquid nitrogen and stored at − 80 °C.

Deglycosylation assays and free-cysteine PEGylation

For protein deglycosylation, yeast membranes were diluted to 2 mg of protein/ml in S-buffer supplemented with 0.1 % (w/v) DDM (n-dodecyl-β-maltoside) (Glycon Biochemicals). After a 5-min pre-incubation on ice, samples were incubated for 30 min on ice in the absence or presence of 0.8 μl of PNGase F (peptide N-glycosidase F) (New England Biolabs). For disulfide bond analysis, total membranes were diluted to 3 mg of protein/ml in S-buffer. Samples were incubated for 20 min at 37 °C with DMSO or mPEG (methoxypolyethylene glycol-5000 maleimide) (Sigma–Aldrich) added from a 10× stock solution in DMSO. For both assays, the reaction was stopped by TCA (trichloroacetic acid) precipitation [34] and samples were resuspended in 18 μl of loading buffer before immunodetection of proteins.

Membrane protein solubilization and pull-down assays

Yeast membranes were diluted to 3 mg of protein/ml in S-buffer supplemented with 0.8 % (w/v) DDM. Samples were gently shaken at 4 °C for 75 min and then cleared of insoluble material by centrifugation at 100000 ***g*** for 1 h at 4 °C. Solubilized yeast membranes were subjected to FLAG-affinity chromatography to recover wild-type ALA2–ALIS5 or mutant ALA2–alis5 complexes. To this end, 200 μl of anti-FLAG® M2 Affinity Gel (Sigma–Aldrich) were washed twice with W-buffer [same as S-buffer but containing 2 % (v/v) glycerol and 0.05 % (w/v) DDM] and subsequently mixed with 9 ml of the detergent-solubilized membrane extract. After incubation with gentle shaking at 4 °C for 18 h, the gel was washed three times with W-buffer. For protein elution, the gel was incubated twice at 4 °C for 30 min with W-buffer supplemented with 400 μg/ml FLAG® peptide (Sigma–Aldrich). Eluates were pooled and concentrated to 250 μl using Vivaspin™ columns (GE Healthcare) with a molecular mass cut-off of 30 kDa.

Protein immunodetection and quantification

Concentrated eluates from the FLAG purification and 60 μl samples of the detergent-solubilized membranes (input controls) were precipitated with TCA, and resuspended in 80 μl of loading buffer [60 mM Tris/HCl, pH 6.8, 10 mM DTT, 2 mM EDTA, 0.75 % (w/v) SDS and 2.6 % (w/v) sucrose] for SDS/PAGE. For total yeast membrane samples, 200 μg of total protein was precipitated with TCA and resuspended in the same amount of loading buffer. In all cases, samples (20 μl) in loading buffer were subjected to electrophoretic separation in denaturing SDS/PAGE gels (10 % (w/v) acrylamide) and transferred on to PVDF membranes for immunodetection [34]. ALA2 was probed with a polyclonal KLH (keyhole-limpet haemocyanin)-conjugated antibody raised in rabbit using a 120-day immunization protocol (Open Biosystems). This antibody recognizes a peptide present at the C-terminal end of ALA2 with the amino acid sequence RRSFGPGTPFEFFQSQSR. Target specificity of this antibody was validated by Western blotting using total membranes from yeast bearing an empty vector, or expressing HA (haemagglutinin)-tagged versions of ALA2 or of the related *Arabidopsis* P4-ATPase ALA3 (Supplementary Figure S1). Absence of cross-reaction with pre-immune serum was also confirmed. FLAG-tagged ALIS5 and alis5 mutants were detected using monoclonal mouse antibody anti-FLAG® M2 (Sigma–Aldrich). Polyclonal goat-anti-rabbit and rabbit-anti-mouse secondary antibodies conjugated to alkaline phosphatase (Dako) were used. All antibodies were employed at a 1:5000 dilution except for anti-FLAG (1:1000 dilution). Bands were visualized with the BCIP (5-bromo-4-chloroindol-3-yl phosphate)/NBT (Nitro Blue Tetrazolium) Color Development Substrate (Promega) according to the manufacturer's instructions.

For pull-down assays, purified wild-type ALA2–ALIS5 and ALA2–alis5 mutant complexes were run in parallel. For each complex, an input control of the solubilized membrane fraction used as starting material for purification was included in the same gel. Western blots were scanned after development, and

band intensity was quantified using ImageJ software (NIH). The intensity of the ALA2 band in each purified complex was normalized to the intensity of the ALA2 band in the corresponding input control with solubilized membranes. The same procedure was used to normalize the recovery of wild-type and mutant ALIS5 versions. Then, the ratio between the normalized ALA2 and wild-type ALIS5 signals was calculated and set to 1 as a reference. The ratio between the normalized ALA2 and alis5 signals was similarly calculated and referred to the wild-type value. Results are means for two independent solubilization experiments.

ATPase activity assays

Purified samples from pull-down assays (6.8 μl) supplemented with 5 mM NaN_3were incubated for 20 min at room temperature with 0.32 mg/ml POPC (1-palmitoyl-2-oleoyl-*sn*-glycero-3-phosphocholine) or a mixture of POPC with POPS (1-palmitoyl-2-oleoyl-*sn*-glycero-3-phospho-L-serine) (7:3, v/v) in the presence or absence of 1 mM sodium orthovanadate (Sigma–Aldrich). All lipids were purchased from Avanti Polar Lipids. ATPase activity assays were performed in 50 μl reaction mixtures containing 50 mM Hepes (pH 7.5), 100 mM NaCl, 50 mM KCl, 10 mM $MgCl_2$ and 4 mM Na_2ATP (Sigma–Aldrich). After incubation at 37 °C for 45 min, the reaction was stopped by dilution with 150 μl of phosphate-free water. Released inorganic phosphate was then detected using a Malachite Green assay [3]. Briefly, to samples from the ATPase assay, 150 μl of PiA solution [two volumes of 7.8 % (v/v) H_2SO_4 + one volume of 0.1 M Na_2MoO_4], 150 μl of PiB solution [0.4 mM Malachite Green dye (Sigma–Aldrich) in 1 % (w/v) poly(vinyl alcohol)] and 500 μl of 7.8 % (v/v) H_2SO_4 were added consecutively. After 30 min of incubation at room temperature in the dark, the absorbance was measured at 630 nm. The amount of released inorganic phosphate was calculated on the basis of KH_2PO_4 standards. Results are means for two independent solubilization experiments.

Transient expression in tobacco epidermal leaf cells and confocal microscopy

Agrobacterium tumefaciens strain C58C1 [35] was transformed by electroporation, and transformants were selected on LB plates [1.5 % (w/v) agar, 1.0 % (w/v) tryptone, 0.5 % (w/v) yeast extract and 0.5 % (w/v) NaCl] supplemented with 25 μg/ml gentamicin and 50 μg/ml kanamycin. Transient expression in tobacco epidermal cells was carried out as described in [36] using 3-week-old *Nicotiana benthamiana* plants. To facilitate high expression of recombinant proteins, *Agrobacterium* strains carrying the different constructs were co-infiltrated with a strain carrying the p19 gene encoding the viral p19 protein that specifically inhibits plant post-transcriptional gene silencing [37]. The concentration of each *Agrobacterium* strain in the mixture was adjusted to a D_{600} of 0.03. Cells were visualized 3–4 days after infiltration using a Leica TCS SP2/MP or SP5 II spectral confocal laser-scanning microscope with a ×63 1.2 numerical aperture water-immersion objective as described previously [24].

Protein sequence alignment

Sequences were aligned using T-Coffee software [38]. Accession numbers were: *A. thaliana*, ALIS1 (Q9LTW0), ALIS3 (Q9SLK2) and ALIS5 (Q8L8W0); human, CDC50A (Q9NV96) and CDC50B (Q3MIR4); *S. cerevisiae*, Cdc50p (P25656), Crf1p (P53740) and Lem3p (P42838); *L. infantum*, LiRos1 (A4IBN0), LiRos2 (A4HU24), LiRos3 (A4I7N1); and *C. elegans*, CHAT-1 (H2L0H3).

Sequence-based prediction of post-translationally modified residues

Post-translationally modified residues in the ALIS5 protein sequence were predicted through online prediction servers. N-glycosylation was examined using the NetNGlyc 1.0 Server at http://www.cbs.dtu.dk/services/. The presence of putative disulfide bonds was analysed using the DiANNA 1.1 web server (http://clavius.bc.edu/~clotelab/DiANNA/), the CYSPRED Predictor (http://gpcr.biocomp.unibo.it/cgi/predictors/cyspred/pred_cyspredcgi.cgi) and the SCRATCH protein predictor (http://scratch.proteomics.ics.uci.edu/).

RESULTS

Prediction of post-translationally modified residues in the ALIS5 ectodomain

Sequence-based prediction suggested that the ectodomain of the plant P4-ATPase β-subunit ALIS5 contains 233 amino acids with two putative N-glycosylation sites (Asn^{181} and Asn^{231}) and four cysteine residues (Cys^{86}, Cys^{107}, Cys^{158} and Cys^{172}) (Figure 1). Alignment of the ALIS5 amino acid sequence with those of selected β-subunits from plants, humans, *C. elegans*, yeast and *Leishmania* parasites revealed that glycosylation of the ectodomain at Asn^{231} is specific for ALIS5 (Figure 1). In contrast, glycosylation site Asn^{181} resides in a sequence motif (PCGLVAWSLFND) that is highly conserved among all Cdc50 proteins tested, and which also contains a conserved cysteine residue (Cys^{172} in ALIS5). Of the other three cysteine residues in the ALIS5 ectodomain, Cys^{158} is conserved in all tested β-subunits except *L. infantum* LiRos1, whereas Cys^{107} is not present in any *Leishmania* β-subunit. In contrast, Cys^{86} is characteristic of all three *Arabidopsis* β-subunits. Notably, this cysteine residue is located in a poorly conserved region in which cysteine residues can be found for almost all organisms analysed, but at different positions. The ALIS5 ectodomain sequence was run through several online prediction servers to identify putative disulfide bonds with contradictory results.

Mapping N-glycosylation sites in the ALIS5 ectodomain

To determine whether Asn^{181} and Asn^{231} undergo N-glycosylation *in vivo*, mutant versions of ALIS5 bearing single or double point mutations were generated by replacing these asparagine residues with glutamine (N231Q, N181Q and N231Q/N181Q). Next, we co-expressed the different *alis5* variants with the *ALA2* catalytic subunit in a yeast strain deleted in three out of five endogenous P4-ATPases (*Δdnf1Δdnf2Δdrs2)* [28], taking advantage of the fact that N-glycosylation initiation in the ER is conserved in all eukaryotic cells. Thus, although the final glycan composition is different for a protein expressed in yeast or plants, N-glycosylation takes place at the same positions [39]. Western blot analysis of total yeast membranes demonstrated that mutation of the putative glycosylation sites does not significantly affect protein expression (Figure 2A). Western blot analysis showed two bands of different mobility (approximately 37.5 and 40 kDa) for the wild-type version of ALIS5 (Figure 2B). The high-intensity 40 kDa band (band I) corresponded to a glycosylated form of the protein, as demonstrated by the loss of signal intensity for this band after glycosidase incubation. The low-intensity 37.5 kDa band

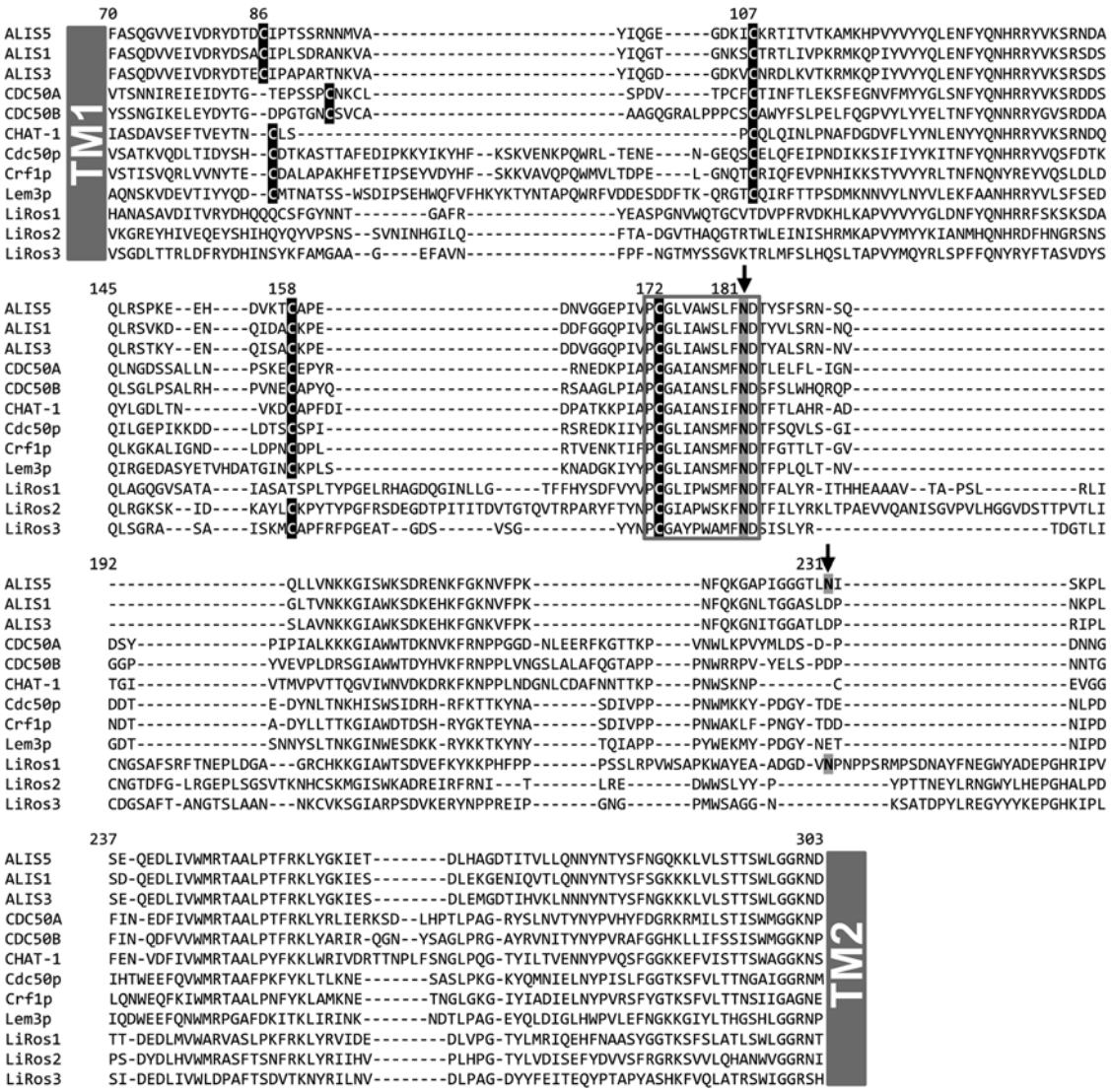

Figure 1 Alignment of the ectodomain of Ccd50 proteins

Amino acid sequences from Cdc50 proteins described to interact with P4-ATPases in *A. thaliana* (ALIS, ALIS3 and ALIS5), humans (CDC50A and CDC50B), *C. elegans* (CHAT-1), *S. cerevisiae* (Cdc50p, Lem3p and Crf1p) and *L. infantum* (LiRos1, LiRos2 and LiRos3) were aligned using T-Coffee. Accession numbers are listed in the Materials and methods section. Only the part of the alignment corresponding to the ALIS5 ectodomain is shown. Black boxes indicate highly conserved cysteine residues (C). N-glycosylated residues (N) are shadowed in grey and marked by an arrow. The ALIS5 transmembrane domains (TM) are indicated by grey boxes. All position numbers are given with respect to ALIS5.

(band III) was insensitive to glycosidase digestion even after 60 min of treatment (results not shown), and thus corresponded to non-glycosylated ALIS5. The reduction in signal intensity for the high-molecular-mass band I after glycosidase digestion was accompanied by an increase in the signal for the non-glycosylated band III and the appearance of an intermediate-molecular-mass band (band II), suggesting that more than one glycosylation site is present in the protein. In line with this notion, both *alis5* single mutants (N231Q and N181Q) lacked band I, but showed the intermediate-molecular-mass band II, which was readily deglycosylated by glycosidase treatment. Simultaneous mutation of both predicted glycosylation sites resulted in an intense band corresponding to the non-glycosylated form of ALIS5 (band III) and a weak band of higher molecular mass that is insensitive to PNGase F treatment. Collectively, these results demonstrate that Asn^{181} and Asn^{231} are the only N-glycosylation sites present in ALIS5.

N-glycosylation of ALIS5 is important for functionality and stability of the P4-ATPase complex

Next, the effect of eliminating N-glycosylation in the ALIS5 ectodomain on the function of the P4-ATPase complex was investigated. As a first approach, complementation assays on plates containing cytolytic peptides were performed. The lipid-uptake defect of *Δdnf1Δdnf2Δdrs2* yeast cells results in PS and PE (phosphatidylethanolamine) exposure to the outer leaflet of the plasma membrane. Such abnormal lipid distribution can be detected using the toxic peptides duramycin and papuamide A, which induce lysis of the yeast cells upon binding to cell surface-exposed PE and PS respectively [40,41]. Co-expression of an active P4-ATPase complex in the *Δdnf1Δdnf2Δdrs2* strain recovers membrane lipid asymmetry and thus results in lower sensitivity to the cytotoxic peptides [23,24]. Co-expression of wild-type *ALIS5* with *ALA2* recovered growth in

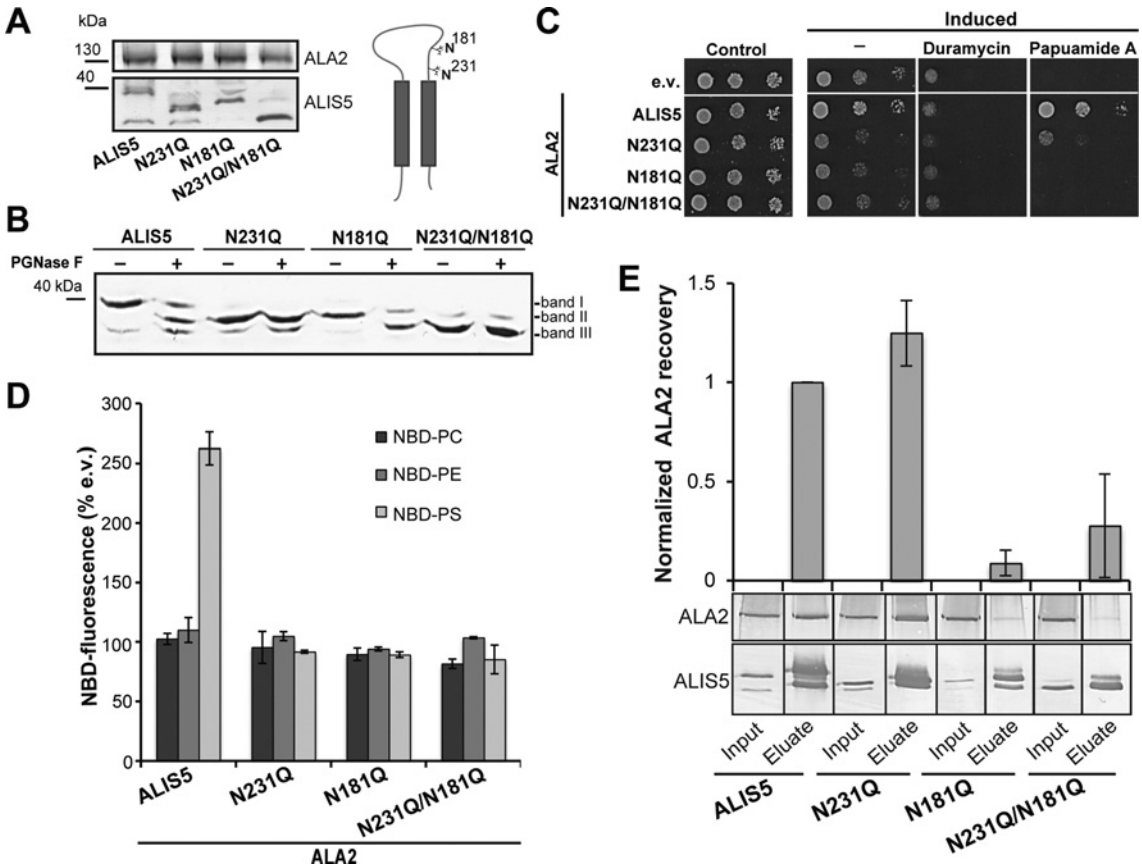

Figure 2 N-glycosylation of the ALIS5 ectodomain is essential for functionality of the P4-ATPase complex

Yeast *Δdnf1Δdnf2Δdrs2* mutant cells were transformed with galactose-inducible plasmids expressing *ALA2* together with FLAG-tagged *ALIS5* or *alis5* N-glycosylation mutants. (**A**) Western blot analysis of total yeast membranes. ALA2 and ALIS5 were detected using anti-ALA2 and anti-FLAG antibodies respectively. Molecular masses are indicated in kDa. (**B**) Yeast membranes were incubated for 30 min in the presence (+) or absence (−) of PNGase F and analysed by immunoblotting. The position of the 40 kDa band is indicated. (**C**) Cells were spotted on to galactose-containing plates (Induced) in the presence or absence (−) of lipid-binding cytotoxic peptides, as indicated. Cells transformed with an empty vector (e.v.) served as a negative control. (**D**) NBD-lipid-uptake assays. Results are normalized to an empty vector (e.v.) control and expressed as means ± S.E.M. from three independent experiments. 100 % corresponds to 64 ± 3 for NBD-PC, 53 ± 4 for NBD-PE and 122 ± 7 for NBD-PS. (**E**) Interaction of ALA2 with wild-type ALIS5 or the indicated alis5 mutants monitored by pull-down assay. Recovery of ALA2 was determined from the quantification of at least two independent experiments as described in the Materials and methods section. Results are means ± S.D.

the presence of papuamide A, but not duramycin (Figure 2C), confirming functional PS transport [24]. Analysis of glycosylation mutants showed that only alis5N231Q was able to promote growth on papuamide A, although at a reduced level compared with wild-type ALIS5 (Figure 2C). These differences in yeast growth could not be related to variations in expression levels between wild-type ALA2–ALIS5 and the different ALA2–alis5 mutant complexes (Figure 2A), suggesting that N-glycosylation, especially at Asn^{181}, is crucial for ALA2–ALIS5 complex functionality.

As a second approach, uptake of fluorescent NBD-phospholipids at the plasma membrane was measured. This assay confirmed that the ALA2–ALIS5 complex internalizes labelled PS but not PE or PC (phosphatidylcholine) [24] (Figure 2D). Disruption of N-glycosylation at Asp^{181} (alis5N181Q and alis5N231Q/N181Q) abolished NBD-PS transport. Even though the ALA2–alis5N231Q complex partially complemented the defect in natural PS transport in *Δdnf1Δdnf2Δdrs2* cells (Figure 2C), it was unable to promote NBD-PS transport at the plasma membrane (Figure 2D). Conceivably, the ALA2–alis5N231Q complex localizes to internal membranes, and thereby helps to generate PS membrane asymmetry along the secretory pathway towards the plasma membrane. Attempts to estimate the amount of ALA2–ALIS5 complex at the plasma membrane level were unsuccessful.

The ability of alis5 glycosylation mutants to form stable complexes with ALA2 was assessed by performing pull-down assays where detergent-solubilized yeast membranes expressing *ALA2* and FLAG-tagged versions of wild-type *ALIS5* or *alis5* mutants were subjected to FLAG-affinity chromatography (Figure 2E). Although disruption of N-glycosylation at Asn^{231} had no impact on the recovery of ALA2 in the eluate, Asn^{181} mutants showed reduced recovery of the catalytic subunit, suggesting that N-glycosylation of this residue is essential for stable association of the complex. A PS-dependent vanadate-sensitive ATPase activity could only be measured for complexes containing wild-type ALIS5 (0.096 ± 0.074 nmol of released phosphate/min) and alis5N231Q (0.103 ± 0.041 nmol of released phosphate/min), but not for alis5 mutants modified in the conserved Asn^{181} residue. However, we did not obtain enough material to reliably normalize the activity values to the amount of ALA2 present in the samples. It therefore cannot be ruled out that lack of ATPase activity for alis5N181Q mutants is due to poor ALA2 recovery.

N-glycosylation of the β-subunit is essential for ALA2–ALIS5 complex trafficking *in planta*

To study whether the mutants are able to support trafficking of the complex *in planta*, we used a tobacco transient expression system. In this system, co-expression of *ALA2* with wild-type *ALIS5* results in exit of the transporter complex from the ER and its localization to vesicular structures (Figure 3). These structures were previously demonstrated to correspond to an enlarged pre-vacuolar compartment by co-localization with a marker protein specific for this compartment [24]. Co-expression of GFP–ALA2 in combination with untagged ALIS5 or alis5N231Q promoted localization of the fluorescently tagged P4-ATPase to enlarged pre-vacuolar compartment structures, although a clear ER signal was detected for the glycosylation mutant. In contrast, when co-expressed with alis5N181Q or alis5N231Q/N181Q, ALA2 was retained in ER-like structures and did not reach the pre-vacuolar compartment. To confirm that lack of ER exit is not due to lack of expression of a β-subunit, we generated C-terminally YFP-tagged versions of the alis5 mutants and co-expressed them in tobacco together with GFP–ALA2 (Supplementary Figure S2). In all cases, YFP fluorescence could be readily detected and co-localized with the signal for GFP–ALA2, confirming that glycosylation of Asn^{181} is essential for P4-ATPase complex trafficking.

Mapping disulfide bonds in the ALIS5 ectodomain

To identify putative disulfide bonds between the four cysteine residues (Cys^{86}, Cys^{107}, Cys^{158} and Cys^{172}) in the ALIS5 ectodomain, single alanine substitutions of each cysteine residue (C86A, C107A, C158A and C172A) were generated and expressed together with ALA2 in the *Δdnf1Δdnf2Δdrs2* yeast strain. Western blot analysis of total yeast membranes demonstrated that the expression levels of ALA2 and ALIS5 are unaffected by mutation of the cysteine residues (Figure 4A). Yeast membranes containing ALA2 and wild-type ALIS5 or alis5 cysteine mutants were treated with mPEG, a maleimide-functional PEG molecule able to covalently bind to free cysteine residues [25]. Western blot analysis revealed a 15 kDa increase in mobility for wild-type ALIS5 after mPEG treatment, corresponding to binding of mPEG to a single cysteine residue (Figure 4B). An alis5ΔC mutant lacking all cysteine residues in the ectodomain showed the same shift in mobility, demonstrating that this single free cysteine residue corresponds to residue 41 present in the cytosolic N-terminus of ALIS5. These results also suggest that all four cysteine residues in the ALIS5 ectodomain are involved in disulfide bond formation and are therefore not available for mPEG labelling. Thus single mutation of any of these cysteine residues would generate an additional free cysteine residue and allow the protein to bind two molecules of mPEG, resulting in an additional shift in the apparent molecular mass of the subunit. However, the C86A and C107A mutations did not result in a band of slower mobility, suggesting that these two residues are not accessible for mPEG labelling due to steric/structural constraints or to their involvement in intermolecular disulfide bonds. In contrast, C158A or C172A point mutations resulted in mPEG adducts with an additional mobility shift compared with wild-type ALIS5 or alis5ΔC (Figure 4B). Interestingly, the mobility shift was found to be different for each of the mutants after mPEG treatment. This was also the case for double alis5C107A/C172A and alis5C107A/C158A mutants. Owing to their proximity, it is conceivable that generation of a highly reactive thiol group at position 172 may affect N-glycan extension at the glycosylated Asn^{181}, resulting in a smaller molecule with higher electrophoretic mobility. Our results suggest that the conserved residues Cys^{158} and Cys^{172} form an intramolecular disulfide bond in the ectodomain of ALIS5, whereas Cys^{86} and Cys^{107} are either not accessible to mPEG labelling or are involved in intermolecular disulfide bonds.

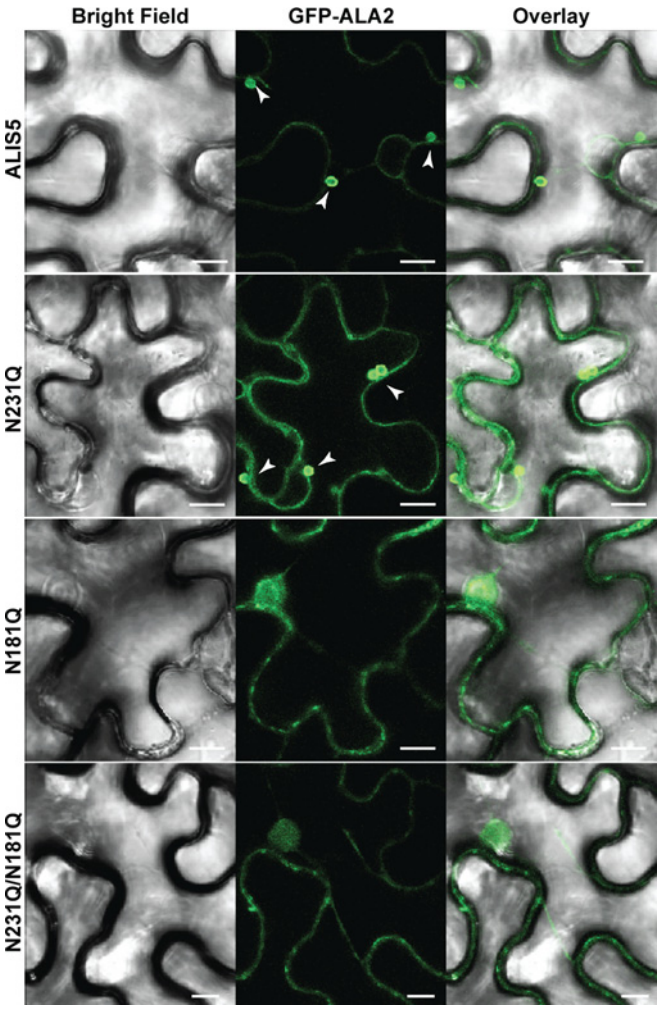

Figure 3 N-glycosylation of Asn^{181} is essential for P4-ATPase complex trafficking

An N-terminal fusion of ALA2 to GFP (GFP–ALA2) was expressed in tobacco leaf epidermal cells in combination with untagged ALIS5 or the indicated alis5 N-glycosylation mutants before imaging by confocal microscopy. Representative images of one experiment out of three are shown. Arrowheads indicate pre-vacuolar compartment structures. Scale bar, 10 μm.

ALIS5 Cys^{86} and Cys^{107} are important for functionality and stability of the P4-ATPase complex

We next investigated the role of disulfide bond formation on functionality of the P4-ATPase complex, by testing the ability of ALA2–alis5 complexes to support growth of the *Δdnf1Δdnf2Δdrs2* yeast strain on papuamide A-containing plates. Co-expression of wild-type *ALIS5* with *ALA2* recovered growth in the presence of papuamide A (Figure 4C). The same was the case for alis5 mutants in Cys^{158} or Cys^{172}, whereas substitution of either Cys^{86} or Cys^{107} failed to support yeast growth. Intriguingly, cells expressing alis5 mutants containing C86A or C107A substitutions presented a general reduction in growth on galactose plates compared with *Δdnf1Δdnf2Δdrs2*

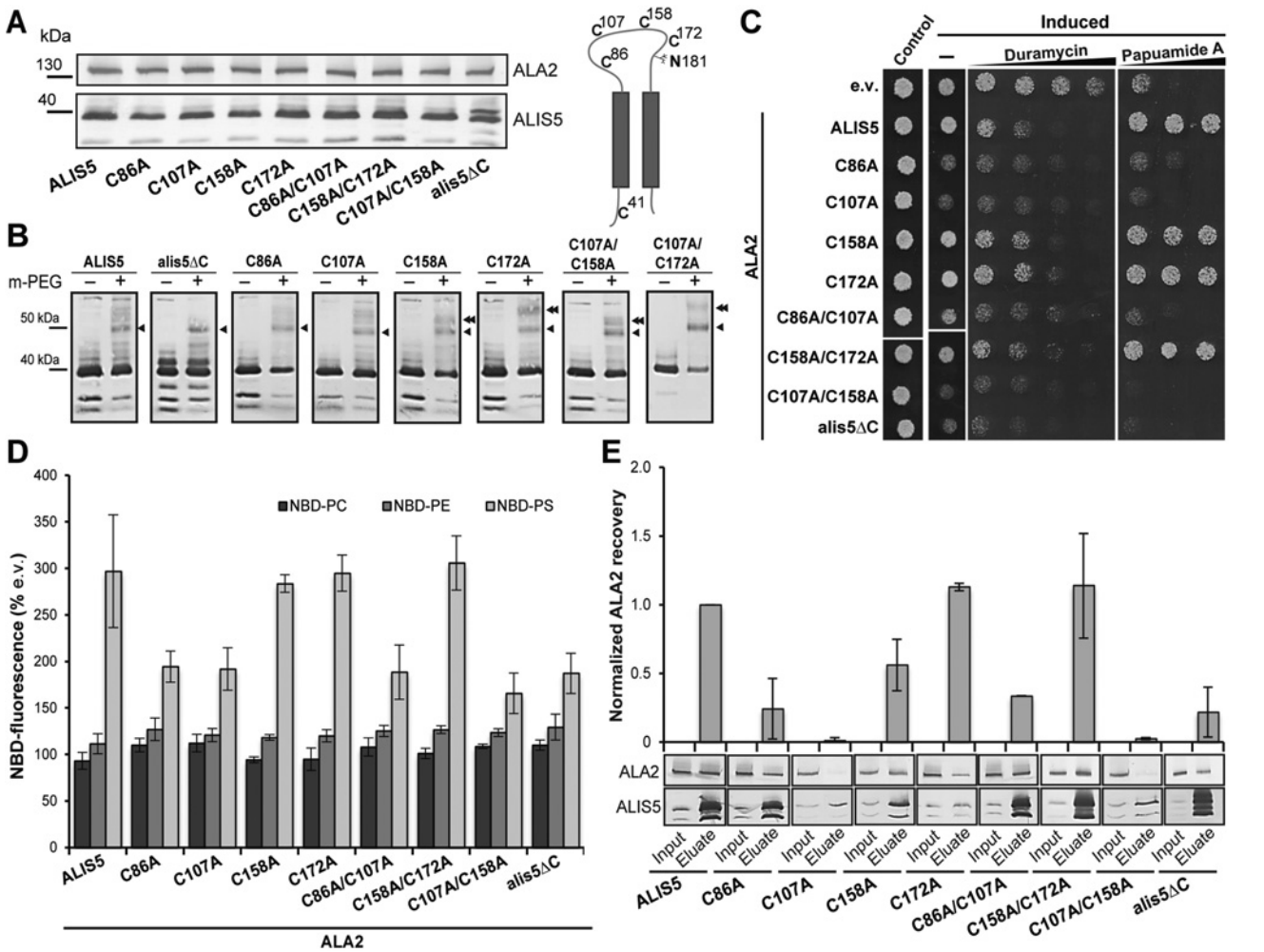

Figure 4 Mutation of Cys^{86} and/or Cys^{107} in ALIS5 disrupts complex association with ALA2

Yeast *Δdnf1Δdnf2Δdrs2* mutant cells were transformed with galactose-inducible plasmids expressing ALA2 together with wild-type ALIS5 or the indicated alis5 mutants carrying cysteine-to-alanine mutations in their ectodomain. (**A**) Western blot analysis of total yeast membranes. ALA2 and ALIS5 were detected using anti-ALA2 and anti-FLAG antibodies respectively. Molecular masses are indicated in kDa. (**B**) Yeast membranes were isolated, incubated in the presence (+) or absence (−) of mPEG and subsequently analysed by Western blotting using anti-FLAG antibody. Arrowheads indicate adducts of ALIS5 bound to one (single arrowheads) or two (double arrowhead) molecules of mPEG. Molecular masses are indicated in kDa. (**C**) Cells were spotted on to galactose-containing plates (Induced) in the presence or absence (−) of lipid-binding cytotoxic peptides, as indicated. Cells transformed with an empty vector (e.v.) served as a negative control. (**D**) NBD-lipid-uptake assays. Results are normalized to empty vector (e.v.) control and expressed as means ± S.D. from at least two independent experiments. 100 % corresponds to 5.8 ± 1.0 for NBD-PC, 5.5 ± 0.6 for NBD-PE and 6.6 ± 0.9 for NBD-PS. (**E**) Interaction of ALA2 with wild-type ALIS5 or the indicated alis5 mutants monitored by pull-down. Recovery of ALA2 was determined from the quantification of at least two independent experiments as described in the Material and methods section. Results are means ± S.D.

cells harbouring an empty vector. This might indicate that these point mutations result in release of a reactive cysteine residue with toxic effects for the cell.

Next, we measured NBD-lipid translocation across the plasma membrane. In line with the growth assay, mutation of cysteine residues involved in confirmed disulfide bond formation (C158A and/or C172A) did not affect NBD-PS lipid transport by the complex (Figure 4D). Surprisingly, albeit to a lesser extent compared with wild-type ALIS5, all alis5 mutants containing C86A or C107A substitutions were still able to transport NBD-PS across the yeast plasma membrane in the presence of ALA2, indicating that these mutations still allow to some extent trafficking of functional complexes to the yeast plasma membrane.

Pull-down assays demonstrated that disruption of the disulfide bond formed between the heavily conserved Cys^{158} and Cys^{172} residues had no impact on complex association (Figure 4E). In contrast, alis5 mutants containing an alanine substitution for Cys^{86} and/or Cys^{107} showed a reduction in the recovery of the ALA2 catalytic subunit with respect to wild-type ALIS5, suggesting that mutation of these residues affects the capacity of the β-subunit to interact with the P4-ATPase.

Cysteine-to-alanine substitutions in the ALIS5 ectodomain do not affect P4-ATPase complex localization *in planta*

Localization of the P4-ATPase complexes was tested by transient expression in tobacco epidermal cells. None of the alis5 cysteine mutations prevented trafficking of ALA2 to the pre-vacuolar compartment (Figure 5). Together with the results of our pull-down assays, these results suggest that the disulfide bond formed between the two evolutionarily conserved cysteine residues in the ALIS5 ectodomain is not essential for association with the catalytic subunit, trafficking or activity of the P4-ATPase complex.

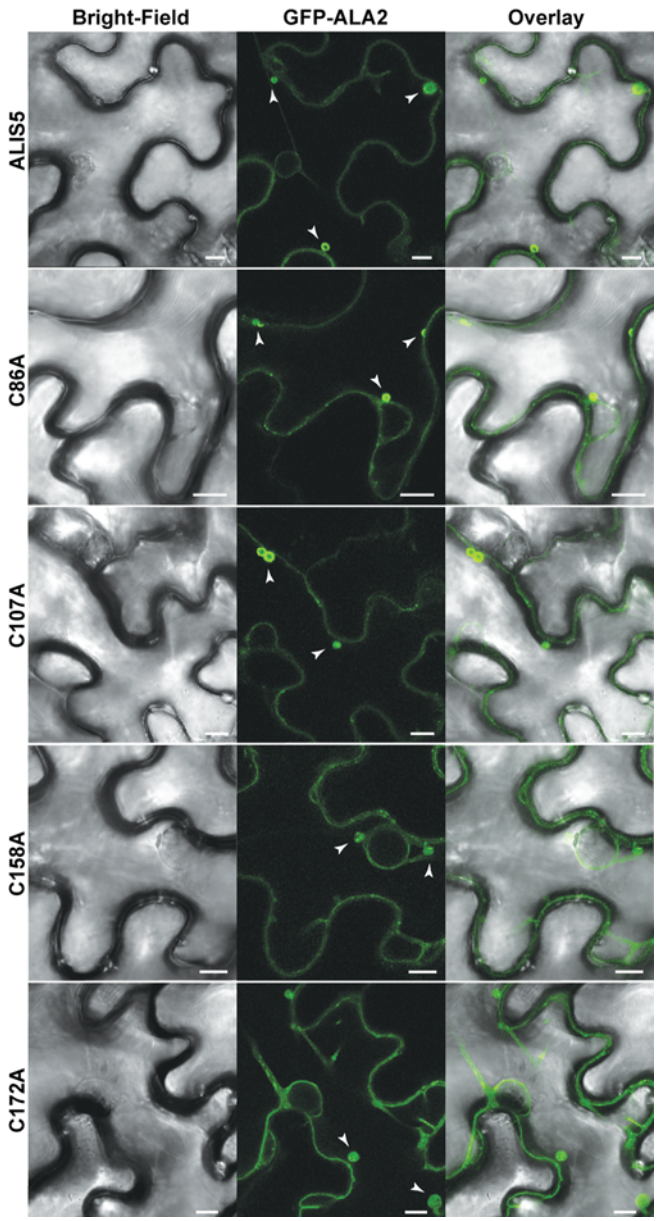

Figure 5 Cysteine residues in the ALIS5 ectodomain are not essential for ALA2 intracellular trafficking

An N-terminal fusion of ALA2 to GFP (GFP–ALA2) was expressed in tobacco leaf epidermal cells in combination with untagged ALIS5 or alis5 cysteine-to-alanine mutants before imaging by confocal microscopy. Representative images of one experiment out of three are shown. Arrowheads indicate pre-vacuolar compartment structures. Scale bar, 10 μm.

In contrast, Cys^{86} and Cys^{107} are required for stable complex association, although mutants of these residues are still able to support, to some extent, trafficking of the P4-ATPase complex and P4-ATPase lipid translocation.

DISCUSSION

In the present study, we verified the presence of post-translationally modified residues in the plant P4-ATPase β-subunit ALIS5, and analysed further the impact of site-directed mutagenesis of these residues in complex assembly, trafficking and functionality. First, we focused on the two predicted glycosylation sites for this protein. N-glycosylation of the conserved residue Asn^{181} in the ALIS5 ectodomain plays an essential role in complex formation and ER exit. In contrast with our results, mutation of this residue in the human P4-ATPase β-subunit CDC50A results in lower expression levels for the rod outer segment P4-ATPase ATP8A2 expressed in HEK (human embryonic kidney)-293 cells [21], but does not affect complex formation, as ATP8A2 can be co-immunoprecipitated with the β-subunit even after elimination of all N-glycosylation sites in CDC50A. In the unicellular parasite *L. infantum*, modification of the same conserved N-glycosylated residue in the β-subunit LiRos3 had no significant effect on the amount of P4-ATPase complex that reached the parasite plasma membrane [27]. This would suggest that, as for the human protein, elimination of glycosylation in the conserved residue does not affect protein interaction within the complex, which is required for ER exit. Interestingly, both ATP8A2 and the *Leishmania* P4-ATPase LiMT specifically interact with CDC50A and LiRos3 respectively, and they do not associate with other β-subunits [11,20]. In contrast, all *Arabidopsis* P4-ATPases characterized to date, including ALA2, are able to interact with any of three different ALIS β-subunits for ER exit [22–24,42]. Although the results obtained in the present study might reflect a plant-specific event, a number of human P4-ATPases are also capable of interacting with several CDC50 proteins [7]. An intriguing possibility to consider is that post-translational modification of the conserved N-glycosylated residue might serve different functions when the β-subunit forms complexes with promiscuous or monogamous members of the P4-ATPase family.

Mutagenesis of the four cysteine residues present in the ectodomain of ALIS5 demonstrated the existence of at least one disulfide bond (Cys^{158}–Cys^{172}), formed between two cysteine residues which seem to be strictly conserved in a number of organisms. Disruption of this disulfide bond in ALIS5 does not have any detrimental effects on P4-ATPase complex interaction, trafficking or lipid translocation across the yeast plasma membrane. This was not expected, as mutation of any of the conserved cysteine residues forming this bond in the yeast β-subunit Lem3p results in a reduction of NBD-lipid internalization at the plasma membrane level [25]. In contrast, mutation of Cys^{86} and/or Cys^{107} in ALIS5 had dramatic effects on stable association of the P4-ATPase complex, as could be inferred from pull-down assays. However, ALA2 was still capable of leaving the ER and making it to the pre-vacuolar compartment when expressed in plant cells together with the alis5C86A and alis5C107A mutants. This suggests that the proteins can still interact at the ER level, but the strength of the interaction within the complex is greatly reduced. Similar results were obtained for yeast Lem3p after mutation of the corresponding cysteine residues [25]. Notably, yeast Lem3p specifically interacts with the plasma membrane P4-ATPases Dnf1p and Dnf2p, and these ATPases do not interact with any other β-subunit [19]. Taken together, our results suggest that the presence of two disulfide bonds within the P4-ATPase β-subunit, one of them located within the first third of the ectodomain, is essential to maintain its functionality. Although the role of this first disulfide bond seems to be conserved between β-subunits for monogamous and promiscuous P4-ATPases, the heavily conserved disulfide bond has evolved slightly different functions.

In conclusion, we have demonstrated the presence of two N-glycosylation sites and at least one disulfide bond in the ectodomain of the plant P4-ATPase β-subunit ALIS5. In contrast with other organisms, elimination of a conserved N-glycosylation site and non-conserved cysteine residues in ALIS5 affects complex formation, whereas elimination of a conserved disulfide

bond does not have any consequence for P4-ATPase complex functionality. The ALA2 P4-ATPase analysed in the present study is a promiscuous protein that interacts with several β-subunits in contrast with previously studied P4-ATPases from other organisms. Although we cannot rule out the possibility that the observed behaviour for the ALA2–ALIS5 complex in the yeast expression system might differ when assayed in the plant native environment, our results suggest that conserved post-translational modifications in the β-subunit might have different roles depending on the promiscuous nature of the interacting P4-ATPase. It would therefore be interesting to investigate whether promiscuous human P4-ATPases react to post-translational modifications in the β-subunit in the same way as the previously characterized monogamous ATP8A2.

AUTHOR CONTRIBUTION

Sara Costa designed and performed all experiments not specifically noted below. Magdalena Marek performed the lipid uptake assays for the alis5 glycosylation mutants and contributed to the plant subcellular localization of ALA2 in the presence of these mutants. Kristian Axelsen contributed with alignment of the β-subunits. Lisa Theorin designed and Sara Costa optimized the purification protocol for ALA2–ALIS5 complexes. Thomas Pomorski and Rosa López-Marqués supervised the project. Sara Costa, Thomas Pomorski and Rosa López-Marqués wrote the paper with the input of other authors.

ACKNOWLEDGEMENTS

We thank Sonja Beers for excellent technical assistance and Professor Michael Palmgren for stimulating discussion and enthusiastic support. Imaging data were collected at the Center for Advanced Bioimaging Denmark (CAB), University of Copenhagen.

FUNDING

This project was funded by Danish Council for Strategic Research (FungalFight project), the Danish National Research Foundation (Center of Excellence PUMPKIN) [grant number DNRF85] and the Danish Council for Independent Research Natural Sciences (FNU) [project number 10-083406]. KBA is funded by the Swiss Federal Government through the State Secretariat for Education, Research and Innovation (SERI).

REFERENCES

1 Palmgren, M.G. and Nissen, P. (2011) P-Type ATPases. Annu. Rev. Biophys. **40**, 243–266 CrossRef PubMed
2 Axelsen, K.B. and Palmgren, M.G. (1998) Evolution of substrate specificities in the P-type ATPase superfamily. J. Mol. Evol. **46**, 84–101 CrossRef PubMed
3 Pomorski, T. (2003) Drs2p-related P-type ATPases Dnf1p and Dnf2p are required for phospholipid translocation across the yeast plasma membrane and serve a role in endocytosis. Mol. Biol. Cell **14**, 1240–1254 CrossRef PubMed
4 De La Hera, D.P., Corradi, G.R., Adamo, H.P. and De Tezanos Pinto, F. (2013) Parkinson's disease-associated human P_{5B}-ATPase ATP13A2 increases spermidine uptake. Biochem. J. **450**, 47–53 CrossRef PubMed
5 Puts, C.F. and Holthuis, J.C.M. (2009) Mechanism and significance of P-4 ATPase-catalyzed lipid transport: lessons from a Na^+/K^+-pump. Biochim. Biophys. Acta **1791**, 603–611 CrossRef PubMed
6 Geering, K. (2008) Functional roles of Na,K-ATPase subunits. Curr. Opin. Nephrol. Hypertens. **17**, 526–532 CrossRef PubMed
7 Bryde, S., Hennrich, H., Verhulst, P.M., Devaux, P.F., Lenoir, G. and Holthuis, J.C.M. (2010) CDC50 proteins are critical components of the human class-1 P4-ATPase transport machinery. J. Biol. Chem. **285**, 40562–40572 CrossRef PubMed
8 Paulusma, C.C., Folmer, D.E., Ho-Mok, K.S., de Waart, D.R., Hilarius, P.M., Verhoeven, A.J. and Oude Elferink, R.P.J. (2007) ATP8B1 requires an accessory protein for endoplasmic reticulum exit and plasma membrane lipid flippase activity. Hepatology **47**, 268–278 CrossRef
9 Saito, K. (2004) Cdc50p, a protein required for polarized growth, associates with the Drs2p P-type ATPase implicated in phospholipid translocation in *Saccharomyces cerevisiae*. Mol. Biol. Cell **15**, 3418–3432 CrossRef PubMed
10 Poulsen, L.R., Lopez-Marques, R.L., McDowell, S.C., Okkeri, J., Licht, D., Schulz, A., Pomorski, T., Harper, J.F. and Palmgren, M.G. (2008) The *Arabidopsis* P4-ATPase ALA3 localizes to the Golgi and requires a β-subunit to function in lipid translocation and secretory vesicle formation. Plant Cell **20**, 658–676 CrossRef PubMed
11 Pérez-Victoria, F.J., Sánchez-Cañete, M.P., Castanys, S. and Gamarro, F. (2006) Phospholipid translocation and miltefosine potency require both *L. donovani* miltefosine transporter and the new protein LdRos3 in *Leishmania* parasites. J. Biol. Chem. **281**, 23766–23775 CrossRef PubMed
12 Vagin, O., Turdikulova, S. and Sachs, G. (2005) Recombinant addition of N-glycosylation sites to the basolateral Na,K-ATPase β1 subunit results in its clustering in caveolae and apical sorting in HGT-1 cells. J. Biol. Chem. **280**, 43159–43167 CrossRef PubMed
13 Laughery, M.D., Todd, M.L. and Kaplan, J.H. (2003) Mutational analysis of α–β subunit interactions in the delivery of Na,K-ATPase heterodimers to the plasma membrane. J. Biol. Chem. **278**, 34794–34803 CrossRef PubMed
14 Ueno, S., Kusaba, M., Takeda, K., Maeda, M., Futai, M., Izumi, F. and Kawamura, M. (1995) Functional consequences of substitution of the disulfide-bonded segment, Cys^{127}–Cys^{150}, located in the extracellular domain of the Na,K-ATPase β subunit: Arg^{148} is essential for the functional expression of Na,K-ATPase. J. Biochem. **117**, 591–596 PubMed
15 Lutsenko, S. and Kaplan, J.H. (1993) An essential role for the extracellular domain of the Na,K-ATPase β-subunit in cation occlusion. Biochemistry **32**, 6737–6743 CrossRef PubMed
16 Jacquot, A., Montigny, C., Hennrich, H., Barry, R., le Maire, M., Jaxel, C., Holthuis, J., Champeil, P. and Lenoir, G. (2012) Phosphatidylserine stimulation of Drs2p-Cdc50p lipid translocase dephosphorylation is controlled by phosphatidylinositol 4-phosphate. J. Biol. Chem. **287**, 13249–13261 CrossRef PubMed
17 Lopez-Marques, R.L., Theorin, L., Palmgren, M.G. and Pomorski, T.G. (2014) P4-ATPases: lipid flippases in cell membranes. Pflügers Arch. **466**, 1227–1240 CrossRef
18 Paulusma, C.C. and Oude Elferink, R.P.J. (2010) P4 ATPases: the physiological relevance of lipid flipping transporters. FEBS Lett. **584**, 2708–2716 CrossRef PubMed
19 Noji, T., Yamamoto, T., Saito, K., Fujimura-Kamada, K., Kondo, S. and Tanaka, K. (2006) Mutational analysis of the Lem3p-Dnf1p putative phospholipid-translocating P-type ATPase reveals novel regulatory roles for Letn3p and a carboxyl-terminal region of Dnf1p independent of the phospholipid-translocating activity of Dnf1p in yeast. Biochem. Biophys. Res. Commun. **344**, 323–331 CrossRef PubMed
20 van der Velden, L.M., Wichers, C.G.K., van Breevoort, A.E.D., Coleman, J.A., Molday, R.S., Berger, R., Klomp, L.W.J. and van de Graaf, S.F.J. (2010) Heteromeric interactions required for abundance and subcellular localization of human CDC50 proteins and class 1 P-4-ATPases. J. Biol. Chem. **285**, 40088–40096 CrossRef PubMed
21 Coleman, J.A. and Molday, R.S. (2011) Critical role of the β-subunit CDC50A in the stable expression, assembly, subcellular localization, and lipid transport activity of the P4-ATPase ATP8A2. J. Biol. Chem. **286**, 17205–17216 CrossRef PubMed
22 López-Marqués, R.L., Poulsen, L.R. and Palmgren, M.G. (2012) A putative plant aminophospholipid flippase, the *Arabidopsis* P4 ATPase ALA1, localizes to the plasma membrane following association with a β-subunit. PLoS One **7**, e33042 CrossRef PubMed
23 Poulsen, L.R., López-Marqués, R.L., Pedas, P.R., McDowell, S.C., Brown, E., Kunze, R., Harper, J.F., Pomorski, T.G. and Palmgren, M. (2015) A phospholipid uptake system in the model plant *Arabidopsis thaliana*. Nat. Commun. **6**, 7649 CrossRef PubMed
24 López-Marqués, R.L., Poulsen, L.R., Hanisch, S., Meffert, K., Buch-Pedersen, M.J., Jakobsen, M.K., Pomorski, T.G. and Palmgren, M.G. (2010) Intracellular targeting signals and lipid specificity determinants of the ALA/ALIS P4-ATPase complex reside in the catalytic ALA α-subunit. Mol. Biol. Cell **21**, 791–801 CrossRef PubMed
25 Puts, C.F., Panatala, R., Hennrich, H., Tsareva, A., Williamson, P. and Holthuis, J.C.M. (2012) Mapping functional interactions in a heterodimeric phospholipid pump. J. Biol. Chem. **287**, 30529–30540 CrossRef PubMed
26 Kato, U., Emoto, K., Fredriksson, C., Nakamura, H., Ohta, A., Kobayashi, T., Murakami-Murofushi, K., Kobayashi, T. and Umeda, M. (2002) A novel membrane protein, Ros3p, is required for phospholipid translocation across the plasma membrane in *Saccharomyces cerevisiae*. J. Biol. Chem. **277**, 37855–37862 CrossRef PubMed
27 García-Sánchez, S., Sánchez-Cañete, M.P., Gamarro, F. and Castanys, S. (2014) Functional role of evolutionarily highly conserved residues, N-glycosylation level and domains of the *Leishmania* miltefosine transporter-Cdc50 subunit. Biochem. J. **459**, 83–94 CrossRef PubMed
28 Hua, Z. (2002) An essential subfamily of Drs2p-related P-type ATPases is required for protein trafficking between Golgi complex and endosomal/vacuolar system. Mol. Biol. Cell **13**, 3162–3177 CrossRef PubMed
29 Gietz, R.D. and Woods, R.A. (2002) Transformation of yeast by lithium acetate/single-stranded carrier DNA/polyethylene glycol method. Methods Enzymol. **350**, 87–96 CrossRef PubMed

30 Liu, Y., Li, J., Du, J., Hu, M., Bai, H., Qi, J., Gao, C., Wei, T., Su, H., Jin, J. et al. (2011) Accurate assessment of antibiotic susceptibility and screening resistant strains of a bacterial population by linear gradient plate. Sci. China Life Sci. **54**, 953–960 CrossRef PubMed
31 Burgers, P.M.J. (1999) Overexpression of multisubunit replication factors in yeast. Methods **18**, 349–355 CrossRef PubMed
32 Curtis, M.D. and Grossniklaus, U. (2003) A gateway cloning vector set for high-throughput functional analysis of genes *in planta*. Plant Physiol. **133**, 462–469 CrossRef PubMed
33 Earley, K.W., Haag, J.R., Pontes, O., Opper, K., Juehne, T., Song, K. and Pikaard, C.S. (2006) Gateway-compatible vectors for plant functional genomics and proteomics. Plant J. **45**, 616–629 CrossRef PubMed
34 Villalba, J.M., Palmgren, M.G., Berberian, G.E., Ferguson, C. and Serrano, R. (1992) Functional expression of plant plasma membrane H^+-ATPase in yeast endoplasmic reticulum. J. Biol. Chem. **267**, 12341–12349 PubMed
35 Koncz, C. and Schell, J. (1986) The promoter of TL-DNA gene 5 controls the tissue-specific expression of chimaeric genes carried by a novel type of *Agrobacterium* binary vector. Mol. Gen. Genet. **204**, 383–396 CrossRef
36 Poulsen, L.R., Palmgren, M.G. and López-Marqués, R.L. (2016) Transient expression of P-type ATPases in tobacco epidermal cells. Methods Mol. Biol. **1377**, 383–393 CrossRef PubMed
37 Voinnet, O., Rivas, S., Mestre, P. and Baulcombe, D. (2003) An enhanced transient expression system in plants based on suppression of gene silencing by the p19 protein of tomato bushy stunt virus. Plant J. **33**, 949–956 CrossRef PubMed
38 Notredame, C., Higgins, D.G. and Heringa, J. (2000) T-Coffee: a novel method for fast and accurate multiple sequence alignment. J. Mol. Biol. **302**, 205–217 CrossRef PubMed
39 Schwarz, F. and Aebi, M. (2011) Mechanisms and principles of N-linked protein glycosylation. Curr. Opin. Struct. Biol. **21**, 576–582 CrossRef PubMed
40 Märki, F., Hänni, E., Fredenhagen, A. and van Oostrum, J. (1991) Mode of action of the lanthionine-containing peptide antibiotics duramycin, duramycin B and C, and cinnamycin as indirect inhibitors of phospholipase A_2. Biochem. Pharmacol. **42**, 2027–2035 CrossRef PubMed
41 Parsons, A.B., Lopez, A., Givoni, I.E., Williams, D.E., Gray, C.A., Porter, J., Chua, G., Sopko, R., Brost, R.L., Ho, C.-H. et al. (2006) Exploring the mode-of-action of bioactive compounds by chemical-genetic profiling in yeast. Cell **126**, 611–625 CrossRef PubMed
42 McDowell, S.C., López-Marqués, R.L., Poulsen, L.R., Palmgren, M.G. and Harper, J.F. (2013) Loss of the *Arabidopsis thaliana* P4-ATPase ALA3 reduces adaptability to temperature stresses and impairs vegetative, pollen, and ovule development. PLoS One **8**, e62577 CrossRef PubMed

Received 9 March 2016/1 April 2016; accepted 4 April 2016
Accepted Manuscript online 5 April 2016, doi:10.1042/BCJ20160207